Research Journal of Applied Sciences, Engineering and Technology 7(6): 1223-1229, 2014
DOI:10.19026/rjaset.7.384
ISSN: 2040-7459; e-ISSN: 2040-7467

Submitted: March 28, 2013 Accepted: April 15, 2013 Published: February 15, 2014

Research Article

AR-based Algorithms for Short Term Load Forecast

Zuhairi Baharudin, Mohd. Azman Zakariya, Mohd. HarisMdKhir,
Perumal Nallagownden and Muhammad Qamar Raza
Electrical and Electronics Department, Universiti Teknologi PETRONAS,
31750 Tronoh, Perak, Malaysia

Abstract: Short-term load forecast plays an important role in planning and operation of power systems. The accuracy of the forecast value is necessary for economically efficient operation and effective control of the plant. This study describes the methods of Autoregressive (AR) Burg's and Modified Covariance (MCOV) in solving the short term load forecast. Both algorithms are tested with power load data from Malaysian grid and New South Wales, Australia. The forecast accuracy is assessed in terms of their errors. For the comparison the algorithms are tested and benchmark with the previous successful proposed methods.

Keywords: Artificial neural network, Autoregressive (AR), linear predictor, Short Term Load Forecast (STLF)

INTRODUCTION

Short term prediction of future load demand is important for the economic and secure operation of power systems. Fundamental operation functions such as unit commitment, hydro-thermal coordination, interchange evaluation, scheduled maintenance and security assessment require a reliable Short Term Load Forecast (STLF).

Throughout the study the term "short" is used to imply prediction times of the order of hours. The time boundaries are from the next hour, or possibly half-hour, up to 168 h. The basic quantity of interest in STLF is the hourly integrated total system load. Owing to the importance of the STLF, research in this area in the past two decades has resulted in the development of numerous forecasting methods (Chakhchoukh *et al*., 2011; De Felice and Xin, 2011; Del-Carpio Huayllas and Ramos, 2010; Hanmandlu and Chauhan, 2011; Amarawickrama and Hunt, 2008; Baharudin and Kamel, 2007).

One of the STLF methods that received significant attention in literature for more than 20 years and a large number of estimation methods is Autoregressive Integrated Moving Average (ARIMA). The method is also known as Box-Jenkins has more degrees of freedom than the autoregressive, so greater latitude in its ability to generate diverse time-series shapes is therefore, expected of its estimators. Unfortunately, this is not always the case, because of the nonlinear nature required of algorithms that must simultaneously estimate the moving average and autoregressive parameters of the models. This phenomenon finally produces low accuracy in forecast of the model algorithm based from the assumption below:

- Several methods may end up in a hard failure mode.
- Maximum-likelihood methods that depend on search over the parameter space involve significant computations and are not guaranteed to converge, or they may converge to the wrong solution.
- Finally, some methods may be inaccurate (e.g., significantly biased) in finite samples.

Though the all pole models have less degree of freedom, they exhibit major advantages. First of all, all-pole models have been found to provide a sufficiently accurate representation for many different types of signals in many different applications. Another reason for the popularity is the special structure which leads to fast and efficient algorithms for finding the all-pole parameters.

In this study, we use Burg's and the Modified Covariance (MCOV) as AR-based algorithms solution to STLF problem. The methods are introduced and their performance are tested and compared with Box-Jenkins ARIMA (Darbellay and Slama, 2000) and ANN (Baharudin and Kamel, 2008).

ELECTRICAL LOAD DATA IN MALAYSIA GRID AND NEW SOUTH WALES, AUSTRALIA

The features of load series in any particular region between one and another are clearly different. The

Corresponding Author: Zuhairi Baharudin, Electrical and Electronics Department, University Teknologi PETRONAS, 31750 Tronoh, Perak, Malaysia

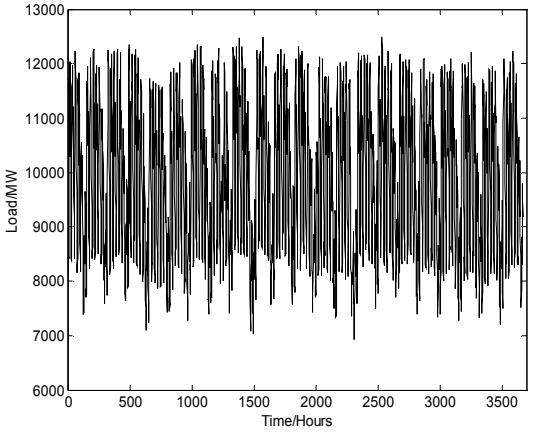

Fig. 1: Historical data for the Malaysian grid from 01 March 2005 to14 August 2005

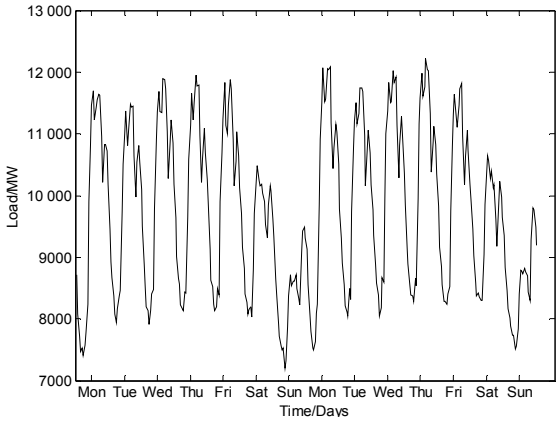

Fig. 2: Hourly load curve for the Malaysian grid for two weeks

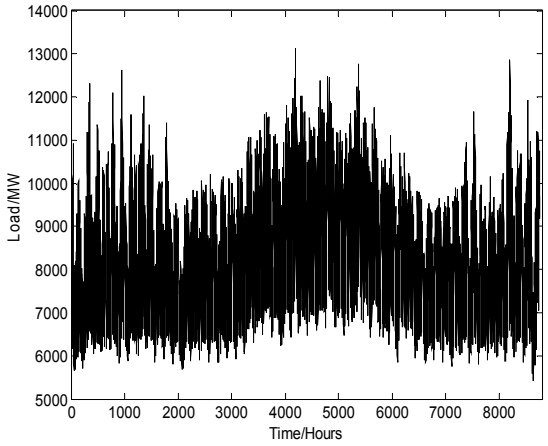

Fig. 3: Historical data for the NSW grid between 01 January 2005 and 31 December 2005

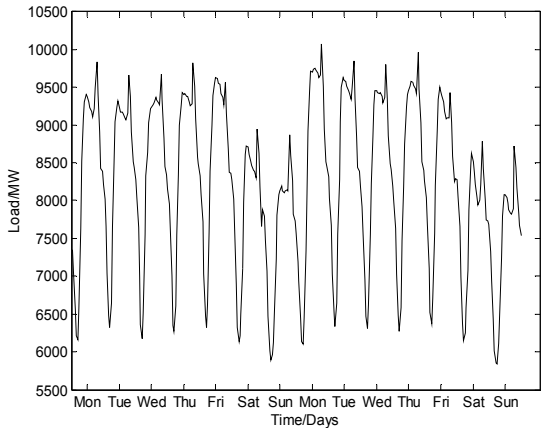

Fig. 4: Hourly load curve for NSW grid for two weeks

significant different can be observed from the aspects of their daily, weekly, monthly and yearly pattern. There are many factors that affect the load series. Two main factors that have been discussed earlier (De la Torre *et al*., 2008; El-Telbany and El-Karmi, 2008; Hyndman and Shu, 2010; Lira *et al*., 2009; Maksimovich and Shiljkut, 2009; Qun *et al*., 2011) that would affect the pattern of load series are economic activities and meteorological variables.

Covering for the Peninsular Malaysia, the Malaysian grid system is operated by Tenaga Nasional Berhad (TNB), supplies the load demand to approximately 20 million people. The lowest demand recorded in 2005 is around 7000 MW. Maximum demand can be reached up to 12500 MW. The average weekday load demand is from 10000 to 10500 MW and for the weekend it is slightly lower. Higher load demand consumption is recorded in the area of Klang Valley (central region), Penang (north region) and Johor Bahru (south region). Figure 1 depicts the hourly consumption for six month from 1 March 2005 to 14 August 2005.

The load series shows a relatively steady behavior over the days of the year. This is mainly because of the absence of seasonal climate changes. The obvious components can be seen such as the weekly seasonal cycle and the influence of public holiday. During this recorded period of load demand, the influence of the meteorological variables is somewhat less. The climate is considered consistent with an average temperature of 30°C and the rain fall during this period is considered normal.

Figure 2 depicts the power load of Malaysian grid over a span of 2 weeks. It focuses on intraday pattern. The figure shows clearly three different load patterns; weekdays (Monday through Friday), Saturdays and Sundays. It also manifests that Saturday load is approximately two-third of the average weekdays load and Sunday is nearly half the average weekdays' load. The reason for the difference in the weekend pattern is that in year of 2005, based on the Malaysian Government regulations, Saturdays were half day work and Sundays were full days off. The maximum and minimum demand normally occurs at 2 P.M. and 5 A.M. respectively.

Figure 3 shows power load variation in New South Wales grid over approximately one year of data record. In the contrary to the Malaysian grid where seasonal effects are marginal, the variation in power load due to seasonal effect is quite clear in NSW.

To observe closely the weekly pattern of NSW grid, the hourly load curve of 2 weeks is depicted in Fig. 4. The figure clearly shows that the weekly power load can be decomposed into two patterns; weekdays (Monday through Friday) and weekends (Saturday through Sunday).

THE AUTOREGRESSIVE (AR) MODELS

A wide-sense stationary autoregressive process of order p is a special case of an ARMA (p, q) process in which $q = 0$. An AR (p) process may be generated by filtering unit variance white noise, $u(n)$ with an all-pole filter of the form:

$$H(z) = \frac{b_q(0)}{1 + \sum_{k=1}^{p} a_p(k) z^{-k}} \quad (1)$$

The autocorrelation sequence of an AR process satisfies the Yule-Walker equations:

$$r_x(k) + \sum_{l=1}^{p} a_p(l) r_x(k-l) = \left| b_q(0) \right|^2 \delta(k) \quad ; \; k \geq 0 \quad (2)$$

where $r_x(k)$ is the autocorrelation sequence of the random process $x(n)$. Writing these equations in matrix form for $k = 1, 2, \ldots, p$, using the conjugate symmetry of $r_{xx}(k)$, we have:

$$\begin{bmatrix} r_x(0) & r_x^*(1) & r_x^*(2) & \cdots & r_x^*(p-1) \\ r_x(1) & r_x(0) & r_x^*(1) & \cdots & r_x^*(p-2) \\ r_x(2) & r_x(1) & r_x(0) & \cdots & r_x^*(p-3) \\ \vdots & \vdots & \vdots & \ddots & \vdots \\ r_x(p-1) & r_x(p-2) & r_x(p-3) & \cdots & r_x(0) \end{bmatrix} \begin{bmatrix} a_p(1) \\ a_p(2) \\ a_p(3) \\ \vdots \\ a_p(p) \end{bmatrix} = - \begin{bmatrix} r_x(1) \\ r_x(2) \\ r_x(3) \\ \vdots \\ r_x(p) \end{bmatrix} \quad (3)$$

Therefore, given the autocorrelation $r_x(k)$ for $k = 0, 1, .., p$ we may solve (3) for the AR coefficients. These equations may be solved recursively using Levinson-Durbin Recursion (Amarawickrama and Hunt, 2008) which led to a number of important discoveries including the lattice filter structure. A close relationship exists between a linear prediction filter and an AR process. If the random process $x(n)$ is generated as an AR (p) process and the order of the linear predictor $m = p$, then the predictor coefficients will be identical to the AR parameters. This relationship is exploited by several algorithms in finding the AR coefficients through linear prediction. Consider the forward linear prediction estimate:

$$\hat{x}^f(n) = -\sum_{k=1}^{p} a_p^f(k) x(n-k) \quad (4)$$

of the sample $x(n)$, where $a^f_p(k)$ is the forward linear prediction coefficients at time index k. The hat ^ is used to denote an estimate and the superscript f is used to denote that this is a forward estimate. The prediction is forward in the sense that the estimate at time index n is based on p samples indexed earlier in time. The complex forward linear prediction error is:

$$e_p^f(n) = x(n) - \hat{x}_p^f(n) \quad (5)$$

has a real variance:

$$\rho^f = \mathrm{E}\left\{ \left| e_p^f(n) \right|^2 \right\} \quad (6)$$

where, $\mathbf{E}\{.\}$ denotes the expected value.

In similar way to forward prediction a backward linear prediction error estimate:

$$\hat{x}_p^b(n) = -\sum_{k=1}^{p} a_p^b(k) x(n+k) \quad (7)$$

may also be formed, in which $a^b_p(k)$ is the backward linear prediction coefficient at time index k. A superscript b is used to tag elements associated with the backward linear prediction estimate. The prediction is backward in the sense that the estimate at time index n is based on m samples indexed later in time. The backward linear prediction error is:

$$e_p^b(n) = x(n-m) - \hat{x}_p^b(n-m) \quad (8)$$

and has real variance:

$$\rho^b = \mathbf{E}\left\{ \left| e_p^b(n) \right|^2 \right\} \quad (9)$$

If the Levinson-Durbin recursion is substituted for $a^f_p(k)$ or $a^b_p(k) = a^{f*}_p(k)$ in definitions (4) and (7) for the forward and backward linear prediction errors, then it is simple to see that:

$$\begin{aligned} e_{j+1}^f(n) &= e_j^f(n) + \Gamma_{j+1} e_j^b(n-1) \\ e_{j+1}^b(n) &= e_j^b(n-1) + \Gamma_{j+1}^* e_j^f(n) \end{aligned} \quad (10)$$

Since the lattice filter provides an alternative parameterization of the all-pole filter, i.e., in terms of

its reflection coefficients, we may also consider formulating the all-pole signal modeling problem as one of finding the reflection coefficients that minimize some error. In the following section we look at two such lattice methods for signal modeling including Burg's method and the modified covariance method.

Burg's method: The method determines the reflection coefficients and can be computed sequentially by minimizing the mean-square of the forward and backward prediction error (Hanmandlu and Chauhan, 2011; Hyndman and Shu, 2010):

$$\varepsilon_j^{fb} = \varepsilon_j^f + \varepsilon_j^b = \mathbf{E}\left\{\sum_{n=j}^{N}\left|e_j^f(n)\right|^2 + \sum_{n=j}^{N}\left|e_j^b(n)\right|^2\right\} \quad (11)$$

Now, we may find the value of the reflection coefficients Γ_j^{fb} that minimizes ε^{fb}_j by setting the derivates of ε^{fb}_j with respect to $(\Gamma_j^{fb})^*$ equal to zero as follows:

$$\frac{\partial}{\partial\left(\Gamma_j^{fb}\right)^*}\varepsilon_j^{fb} = \frac{\partial}{\partial\left(\Gamma_j^{fb}\right)^*}\mathbf{E}\left[\sum_{n=j}^{N}\left\{\left|e_j^f(n)\right|^2 + \left|e_j^b(n)\right|^2\right\}\right] \quad (12)$$
$$= \mathbf{E}\left[\sum_{n=j}^{N}\left\{e_j^f(n)\left[e_{j-1}^b(n-1)\right]^* + \left[e_j^b(n)\right]^* e_{j-1}^f(n)\right\}\right] = 0$$

Substituting the error update equations for e^f_j (n) and $[e^b_j$ (n)$]^*$ which are similar to those given for $e^f_{j+1\,(n)}$ and $[e^b_{j+1}$ (n)$]^*$ in (21) and solving for Γ_j^{fb} we find that the value of Γ_j^{fb} that minimizes ε^{fb}_j is:

$$\Gamma_j^{fb} = -\frac{2\sum_{n=j}^{N} e_{j-1}^f(n)\left[e_{j-1}^b(n-1)\right]^*}{\sum_{n=j}^{N}\left\{\left|e_{j-1}^f(n)\right|^2 + \left|e_{j-1}^b(n-1)\right|^2\right\}} \quad (13)$$

The modified covariance method: In the previous section we described Burg recursion, which finds the reflection coefficients for an AR model by sequentially minimizing the mean of the squared forward and backward prediction errors. In this section we look at the modified covariance method or forward-backward algorithm for AR signal modeling. As with Burg algorithm, the modified covariance method minimizes the mean of the squares of the forward and backward prediction errors:

$$\varepsilon_p^{fb} = \varepsilon_p^f + \varepsilon_p^b \quad (14)$$

The difference, however, between the two approaches is that, in the modified covariance method, the minimization is not performed sequentially. In other words, for a p^{th}-order model, the modified covariance method finds the set of reflection coefficients or, equivalently, the set of transversal filter coefficients $a_p(k)$, that minimize ε^{fb}_p.

To find the filter coefficients that minimizes ε^{fb}_p we set the derivates of ε^{fb}_p with respect to a^*_p (l) equal to zero for $l = 1, 2, \ldots, p$. Since:

$$e_p^f(n) = x(n) + \sum_{k=1}^{p} a_p^f(k)x(n-k) \quad (15)$$

and

$$e_p^b(n) = x(n-p) + \sum_{k=1}^{p} a_p^{f*}(k)x(n-p+k) \quad (16)$$

Then:

$$\frac{\partial\varepsilon_p^{fb}}{\partial a_p^*(l)} = \mathbf{E}\left[e_p^f(n)\frac{\partial\left[e_p^f(n)\right]^*}{\partial a_p^*(l)} + \left[e_p^b(n)\right]^*\frac{\partial e_p^b(n)}{\partial a_p^*(l)}\right] \quad (17)$$
$$= \mathbf{E}\left[e_p^f(n)x^*(n-l) + \left[e_p^b(n)\right]^* x(n-p+l)\right] = 0$$

Substituting Eq. (15) and (16) into (17) and simplifying we find that the normal equations for the modified covariance method are given by:

$$\sum_{k=1}^{p}\left[r_x(l,k) + r_x(p-k,p-l)\right]a_p^f(k) = -\left[r_x(l,0) + r_x(p,p-l)\right];\ l = 1,\ldots,p \quad (18)$$

where,

$$r_x(l,k) = \sum_{n=p}^{N} x(n-k)x^*(n-l) \quad (19)$$

For the modified covariance error we may use the orthogonality condition in (17) to express ε^{fb}_p as follows:

$$\varepsilon_p^{fb} = E\left[e_p^f(n)x^*(n) + \left[e_p^b(n)\right]^* x(n-p)\right] \quad (20)$$

Substituting the expression given in Eq. (15) and (16) for e^f_p (n) and e^b_p (n) and simplifying, we have:

$$\varepsilon_p^{fb} = r_x(0,0) + r_x(p,p) + \sum_{k=1}^{p} a(k)\left[r_x(0,k) + r_x(p,p-k)\right] \quad (21)$$

APPLICATIONS AND RESULTS

Since, the intention is to test the capability of the proposed AR models in modeling power load series, no

Table 1: The duration for the usage data and validation (forecast period)

Grid	Recorder period	Forecast period
Malaysian	07 March 05-12 June 05	13-19 June 05

Table 2: Load comparison and error during the maximum demand of the day

		ARIMA		ANN		Burg		MCOV	
	Actual load	Forecast load (MW)	Error (%)	Forecast load (MW)	Error (%)	Forecast load (MW)	Error (%)	Forecast load (MW)	Error (%)
Mon	11956	12180	1.87	12250	2.46	12063	0.90	12079	1.03
Tue	11988	12155	1.39	11780	-1.74	12040	0.43	12040	0.44
Wed	11767	11890	1.05	11910	1.22	11824	0.49	11807	0.34
Thu	12027	11900	-1.06	11850	-1.47	12066	0.33	12056	0.24
Fri	11867	11900	1.04	12100	1.96	11958	0.77	11962	0.80
Sat	10133	9850	-2.79	9720	-4.08	10230	0.96	10220	0.86
Sun	8915	9300	4.32	9390	5.33	9050	1.51	9045	1.46

attempt has been initially made to reduce its degree of fluctuation through grouping it into different patterns. With the Malaysian grid, 14 weeks of historical data are applied in building the model and one week data are referred to validate the forecast performance. The duration for the usage data and validation period are depicted shown in Table 1.

In the first experiment we obtained the forecasts of AR's models, ARIMA and ANN of the power load of the maximum demand over all days of the considered week (forecast period). The results are shown in Table 2. The error is calculated from the difference between the actual and forecast and it given by:

$$ERROR = \frac{\hat{x}_i - x_i}{x_i} \quad (22)$$

where,
x_i = The actual data
$\hat{x}_i$ = The forecasted value

Table 2 reports the comparison of the load and error with the actual during the time of maximum demand of the day. The simulations are carried out for lead times of one day ahead. For the weekdays the maximum demand occurs at 3 P.M. Mean while for Saturday and Sunday normally occurs at 4 P.M. and 11 P.M. respectively. For all models the errors are satisfactory during the weekdays except on Monday. This is due to the load demand on Monday is normally inconsistent. Thus, the models somehow find it difficult to adapt to get a good accurate forecast. The forecast value for Saturday and Sunday are slightly higher in comparison to the weekdays. Especially on Sunday all models perform in the same manner. For all days during the time when the maximum demand occurs, AR's model (Burg's and MCOV) show the errors that below 2% compared to ARIMA and ANN.

To show the performances of the different techniques in statistical from, the MAPE values over the days of the considered week of forecasts, are calculated and shown in Table 3. The Mean Absolute Percentage Errors (MAPE), calculated from 24 forecasted values, is used as a performance indicator. The MAPE is given by:

Table 3: Mean Absolute Percentage Errors (MAPE) of daily forecast

	MAPE			
	ARIMA	ANN	Burg	MCOV
Mon	2.10	2.58	1.21	1.23
Tue	1.82	2.21	1.17	1.16
Wed	1.67	1.98	1.06	1.01
Thu	1.12	1.78	0.59	0.56
Fri	1.51	1.85	0.88	0.93
Sat	2.86	3.12	1.22	1.24
Sun	3.21	3.79	1.31	1.31
Average	2.04	2.47	1.06	1.06

Table 4: Record and forecast period

Grid	Recorder period	Forecast period
NSW	01 Jan 05-03 April 05	04 April 05-10 April 05

$$MAPE = \frac{1}{24}\sum_{i=1}^{24}\frac{\left|\hat{x}_i - x_i\right|}{x_i} \quad (23)$$

where,
x_i = The actual data
$\hat{x}_i$ = The forecasted value

The forecast results for Burg's and MCOV models clearly outperformed ARIMA (Hanmandlu and Chauhan, 2011) and ANN (Amarawickrama and Hunt, 2008). For the day comparison, the highest error recorded for all models occur on Sunday. Whereas the lowest recorded is on Thursday. Average MAPE is considered sufficient for the Malaysian Grid operator (TNB) for all models. However, Burg's and MCOV models prove that an AR's model is capable to conduct such load forecast with better accuracy.

In the third experiment, we obtained the forecasts for AR's models, ARIMA and ANN for load demand of NSW. The hourly data over 14 weeks in early of the year are applied. Table 4 tabulates the recorded period and the predicted week of the study case.

The experiments are conducted similar of the case for the Malaysia Grid. The first experiment is to obtain the forecast of the maximum demand of the day during the forecast period. Secondly, the 1 day ahead forecast is obtained.

The results for maximum demand and one day ahead forecast are depicted in Table 5 and 6 respectively. Table 5 depicts the comparison of the actual load and forecast with their error during the time

Table 5: Load comparison and error during the maximum demand of the day for NSW

		ARIMA		ANN		Burg		MCOV	
	Actual load	Forecast load (MW)	Error (%)	Forecast load (MW)	Error (%)	Forecast load (MW)	Error (%)	Forecast load (MW)	Error (%)
Mon	9400	9589	2.01	9591	2.03	9320	-0.85	9327	-0.78
Tue	9253	9075	-1.92	9450	2.13	9320	0.72	9322	0.75
Wed	8539	8702	1.91	8750	2.47	8620	0.95	8618	0.93
Thu	8638	8502	-1.57	8480	-1.83	8610	-0.32	8611	-0.31
Fri	9771	9605	-1.70	9590	-1.85	9685	-0.88	9686	-0.87
Sat	9842	10100	2.62	10180	3.43	9978	1.38	9974	1.34
Sun	9845	9985	1.42	9689	-1.58	9794	-0.52	9796	-0.50

Table 6: Mean Absolute Percentage Errors (MAPE) of daily forecast

	MAPE			
	ARIMA	ANN	Burg	MCOV
Mon	2.51	2.85	1.41	1.40
Tue	2.24	2.57	1.25	1.25
Wed	1.92	2.23	1.16	1.15
Thu	1.25	2.03	0.84	0.85
Fri	1.82	2.15	1.02	1.01
Sat	2.96	3.42	1.59	1.58
Sun	2.87	3.12	1.32	1.32
Average	2.22	2.62	1.23	1.22

of maximum demand of the day. The simulations are carried out for lead times of one day ahead similar to Malaysia Grid scenario.

For the simplicity, Table 5 summarizes the maximum demand of the day for 1 week forecast. It can be observed that during the weekdays the maximum demand occurs at 3 P.M. Mean while for Saturday and Sunday it is normally occurs at 4 P.M. and 11 P.M. respectively. For all models the errors are satisfactory during the weekdays except on Monday and Saturday. This is due to the load demand on Monday and Saturday's normally inconsistent. Especially on Saturday, many social and community events take place. Thus, the models somehow find it difficult to adapt to get a good accurate forecast. Unlike the Malaysia Grid the forecast value for Sunday is lower. This is due to the good consistency for the load demand on Sunday in NSW. The fact is true where it can be seen that normally on Sunday less social and community activities are conducted. For all days during the time when the maximum demand occurs, AR's model (Burg's and MCOV) show the errors below 2% compared to ARIMA and ANN.

Once again, the forecast results for Burg's and MCOV models clearly outperformed ARIMA and ANN. For the day comparison, the highest error recorded for all models occur on Sunday. Whereas the lowest recorded is on Thursday. Average MAPE is considered sufficient for the Malaysian Grid operator (TNB) for all models. However, similar to the Malaysia Grid, Burg's and MCOV models prove that an AR's model is capable to conduct such load forecast with better accuracy.

CONCLUSION

In this study, the performance of the univariate Autoregressive (AR) method in short term load forecast is presented. Two AR's models, Burg and the Modified covariance are discussed and used for one-week ahead forecasting with three months power load data record from Malaysian and NSW grid. The performance of Burg and the Modified Covariance (MCOV) is compared with ARIMA and ANN in previous researchers' finding. The comparison results indicate clearly the better performance of the AR-based techniques to the ARIMA and ANN. This could establish the all poles models as an alternative solution to STLF problem.

REFERENCES

Amarawickrama, H.A. and L.C. Hunt, 2008. Electricity demand for Sri Lanka: A time series analysis. Energy, 33(5): 724-739.

Baharudin, Z. and N.S. Kamel, 2007. One week ahead short term load forecasting. Proceeding of the 7th IASTED European Conference on Power and Energy Systems (EuroPES 2007). Palma de Mallorca, Spain, pp: 582-117.

Baharudin, Z. and N.S. Kamel, 2008. A.R. modified covariance in one week ahead short term load forecast. Proceeding of the 2nd IASTED Asian Conference on Power and Energy Systems. Langkawi, Malaysia, pp: 606-070.

Chakhchoukh, Y., P. Panciatici and L. Mili, 2011. Electric load forecasting based on statistical robust methods. IEEE T. Power Syst., 26(3): 982-991.

Darbellay, G.A. and M. Slama, 2000. Forecasting the short-term demand for electricity: Do neural networks stand a better chance? Int. J. Forecasting, 16(1): 71-83.

De Felice, M. and Y. Xin, 2011. Short-term load forecasting with neural network ensembles: A comparative study [Application Notes]. IEEE Comput. Intell. M., 6(3): 47-56.

De la Torre, S., A.J. Conejo and J. Contreras, 2008. Transmission expansion planning in electricity markets. IEEE T. Power Syst., 23(1): 238-248.

Del-Carpio Huayllas, T.E. and D.S. Ramos, 2010. Electric power forecasting methodologies of some south American countries: A comparative analysis. IEEE (Revista IEEE America Latina) Latin Am. T., 8(5): 519-525.

El-Telbany, M. and F. El-Karmi, 2008. Short-term forecasting of Jordanian electricity demand using particle swarm optimization. Electr. Pow. Syst. Res., 78(3): 425-433.

Hanmandlu, M. and B.K. Chauhan, 2011. Load forecasting using hybrid models. IEEE T. Power Syst., 26(1): 20-29.

Hyndman, R.J. and F. Shu, 2010. Density forecasting for long-term peak electricity demand. IEEE T. Power Syst., 25(2): 1142-1153.

Lira, F., C. Munoz, F. Nunez and A. Cipriano, 2009. Short-term forecasting of electricity prices in the colombian electricity market. IET Gener. Transm. Dis., 3(11): 980-986.

Maksimovich, S.M. and V.M. Shiljkut, 2009. The peak load forecasting afterwards its intensive reduction. IEEE T. Power Deliver, 24(3): 1552-1559.

Qun, Z., L. Tesfatsion and L. Chen-Ching, 2011. Short-term congestion forecasting in wholesale power markets. IEEE T. Power Syst., 26(4): 2185-2196.